Choroid, Haller's, and Sattler's Layer Thickness in Intermediate Age-Related Macular Degeneration With and Without Fellow Neovascular Eyes

Marieh Esmaeelpour,[1,2] Siamak Ansari-Shahrezaei,[1] Carl Glittenberg,[1] Susanne Nemetz,[3] Martin F. Kraus,[4] Joachim Hornegger,[4] James G. Fujimoto,[5] Wolfgang Drexler,[2] and Susanne Binder[1]

[1]Ludwig Boltzmann Institute for Retinology and Biomicroscopic Laser Surgery, Department of Ophthalmology, Rudolf Foundation Clinic, Vienna, Austria
[2]Center for Medical Physics and Biomedical Engineering, Medical University Vienna, Vienna, Austria
[3]Optik Nemetz, Vienna, Austria
[4]Pattern Recognition Lab and School of Advanced Optical Technologies, University Erlangen-Nuremberg, Erlangen, Germany
[5]Department of Electrical Engineering and Computer Science, Massachusetts Institute of Technology, Cambridge, Massachusetts, United States

Correspondence: Marieh Esmaeelpour, Department of Ophthalmology, Rudolf Foundation Clinic, Juchgasse 25, 1030 Vienna, Austria; marieh.esmaeelpour@meduniwien.ac.at.

Submitted: April 23, 2014
Accepted: July 5, 2014

Citation: Esmaeelpour M, Ansari-Shahrezaei S, Glittenberg C, et al. Choroid, Haller's, and Sattler's layer thickness in intermediate age-related macular degeneration with and without fellow neovascular eyes. *Invest Ophthalmol Vis Sci*. 2014;55:5074–5080. DOI:10.1167/iovs.14-14646

Purpose. To analyze choroidal, Sattler's, and Haller's layer thickness maps in age-related macular degeneration (AMD) patients having eyes with bilateral large drusen and pigment changes (intermediate AMD), in patients having intermediate AMD eyes with neovascular fellow eyes (nAMD), and in healthy subjects using three-dimensional (3D) 1060-nm optical coherence tomography (OCT).

Methods. Automatically generated choroidal thickness (ChT), retinal thickness, and Sattler's and Haller's layer thickness maps were statistically analyzed in 67 subjects consisting of intermediate AMD ($n = 21$), intermediate AMD ($n = 22$) with fellow nAMD eyes ($n = 22$), and healthy eyes ($n = 24$) with no age and axial eye length difference between groups of eyes ($P > 0.05$, ANOVA). Eyes were imaged by a prototype high-speed (60,000 A-scans/s) spectral-domain 3D 1060-nm OCT over a 36° × 36° field of view.

Results. The mean ± SD (μm) subfoveal ChT for healthy subjects and for bilateral intermediate AMD, unilateral intermediate AMD, and their nAMD fellow eyes was 259 ± 95 and 222 ± 98, 149 ± 60, and 171 ± 78, respectively. Choroidal thickness maps demonstrated significant submacular thinning in unilateral intermediate AMD in comparison to healthy and bilateral intermediate AMD eyes ($P < 0.001$, ANOVA, post hoc $P < 0.001$ and $P < 0.05$, respectively). Sattler's and Haller's layers were thinnest in intermediate AMDs that presented with nAMD fellow eyes (Kruskal-Wallis test $P < 0.01$). For the choroid and its sublayers, there was no difference between the intermediate AMD eyes and their fellow nAMD eyes (paired testing, $P < 0.05$).

Conclusions. The 3D 1060-nm OCT choroidal imaging visualized significant changes in choroidal, Sattler's, and Haller's layer thickness in relation to the progression of AMD. This may be important for understanding the choroidopathy in the pathophysiology of AMD.

Keywords: age-related macular degeneration, optical coherence tomography, choroidal thickness maps, retina, choroid, retina

Late age-related macular degeneration (AMD) has a devastating effect on the central vision, and its prevalence increases exponentially with age.[1–3] Age-related macular degeneration with choroidal neovascularization (nAMD) is a common form of late AMD that can be visualized for diagnosis purposes by angiography.[4–6] Three-dimensional (3D) optical coherence tomography (OCT) is important for noninvasive imaging of the retina and choroid in AMD.[7,8] In recent years, it has been used to investigate choroidal involvement in the development of AMD.[9–12] Physiological aging decreases choroidal thickness,[10,11] but late-stage AMD such as geographic atrophy and nAMD is associated with further choroidal thickness decrease.[12,13] The choroid supplies the outer retina with nutrition and oxygen and is essential for the macular blood supply.[5] Choroidal vasculature is subdivided into small vessels in the choriocapillaris, medium-sized vessels in the Sattler's layer, and large-sized vessels in the Haller's layer. Of the three sublayers, the choriocapillaris has been more closely investigated due to its location adjacent to Bruch's membrane and the photoreceptors and due to its prominent dropout that accompanies geographical atrophy.[14–16]

The pathophysiology of choroidal thinning, its progression from normal aging thinning to AMD-related thinning and the structure of the Sattler's and Haller's layer, need further investigation. Early AMD presenting with small drusen and pigmentary changes may not be associated with choroidal

thickness decrease,[9] although choriocapillaris dropout has been shown in relation to drusen density in early AMD.[17] Large drusen indicate an intermediate form of AMD and are associated with increased the risk of developing nAMD,[18–20] but their relationship with choroidal thickness and the vascular sublayers of Sattler's and Haller's has not been established. Further, OCT at the light source wavelength of 1060 nm may improve the quality of findings, as this wavelength allows measurement over a large field of view and the inclusion of eyes with cataracts; it also provides choroidal penetration independent of signal decrease with depth.[21,22] The present study investigated choroidal, Sattler's, and Haller's layer thickness in eyes with bilateral intermediate AMD and those with intermediate AMD with nAMD in the fellow eye and makes comparisons to healthy eyes. Choroidal thickness maps were statistically analyzed with regard to the distribution of choroidal thickness (ChT) and the severity of AMD as defined by Ferris et al.[23]

Methods

Study Population

Ethical approval was obtained prospectively from the Institutional Review Board, The Ethical Commission of Vienna. Written informed consent was obtained from the subjects after explanation of the nature and possible consequences of the study prior to enrollment. The research adhered to the tenets of the Declaration of Helsinki.

Seventy-four subjects (Caucasians, 54 females and 20 males) were selected based on the inclusion and exclusion criteria as assessed by the medical and ocular history, clinical investigation including indirect ophthalmoscope fundus examination by a medical retina specialist, and if available angiographic findings and best-corrected visual acuity measured with an Early Treatment Diabetic Retinopathy Study (ETDRS) chart. The overall inclusion criterion was age $\geq$ 60 years. Exclusion criteria were subretinal deposits (also termed subretinal drusenoid deposits and reticular pseudodrusen); geographical atrophy involving the center of the macula and focal atrophy larger than 375 μm; acquired vitelliform lesions; eyes treated with anti-vascular endothelial growth factor injections; terminal AMD in the fellow eye; polypoidal AMD; myopia $>$ 6 diopters; history of glaucoma; retinopathy due to epiretinal membranes; any cause of media opacities resulting in impaired visualization of the macula; systemic diabetic disease; smoking; and systemic acute inflammatory or infectious disease. Criteria were assessed both during the selection process and after recruitment on infrared and OCT images. After recruitment, seven patients were excluded based on OCT imaging analysis due to the presence of subretinal deposits (all seven) and acquired vitelliform lesions (one of the seven). These were unnoticed during the clinical investigation and selection process.

Study eyes were grouped into eyes from patients with bilateral intermediate AMD, those having intermediate AMD with nAMD in the fellow eye, and healthy eyes. Healthy eyes were defined as one randomly chosen study eye from subjects with two healthy eyes with no apparent or physiological retinal aging changes on ophthalmologic fundus examination and were included if visual acuity decrease could be explained only by the presence of cataracts. Age-related macular degeneration patients had bilateral intermediate AMD according to the current clinical classification[23] or one eye with intermediate AMD and a fellow eye with nAMD. Intermediate AMD was defined as nonneovascular and by the presence of at least one large drusen $\geq$ 125 μm within two disc diameters of the fovea, with or without pigment changes. Eyes with neovascular changes or suspected of neovascularization were subjected to fluorescein angiography and, if clinically indicated, to indocyanine green angiography. Only one eye from patients with bilateral intermediate AMD was analyzed. Eyes with intermediate AMD and choroidal neovascularization (CNV) secondary to AMD on the fellow eye were grouped separately. All nAMD eyes enrolled in the present study were classified according to the clinical and, if available, the angiographic findings (nonneovascular AMD; nAMD including classic, minimal classic, and occult CNV; and retinal angiomatous proliferation).[24] The resulting groups did not differ in age and axial eye length ($P >$ 0.05, one-way ANOVA, Table).

OCT Imaging

High-speed, 60,000 A-scans/s 3D OCT imaging at 1060 nm was performed with less than 2.5 mW at the cornea, well below the maximum power limit for 10-second exposure,[25,26] with a spectral-domain (SD) OCT prototype.[27] Three-dimensional OCT volumes were acquired at 1060-nm wavelength with 15- to 20-μm transverse resolution, approximately 7-μm axial resolution, and 512 voxels per depth scan (A-scan). Raster scans across a 36° $\times$ 36° field were centered on the fovea and resulted in up to 120 frames/s. System specifications for the 3D 1060-nm OCT were ~97 dB signal-to-noise ratio and their roll-off with scanning depth of 6 dB at ~1.1-mm, ~6- to 7-μm axial resolution, and 2.6-mm scanning depth. Images were processed and registered for eye movements, denoising, and contrast improvement.[28,29]

Choroidal Thickness Maps for Individual Eyes

For the investigation of the ChT variation throughout the entire field of view, ChT maps were generated based on automatic segmentation.[30] Automatic retinal and choroidal segmentation, automatic measurement of subfoveal ChT, and the generation of thickness maps were used for this purpose and are described elsewhere.[21,30] Briefly, this method determines the segmentation line in a low-signal, noisy environment such as in OCT tomograms in the region of the choroid independent of boundary edge information. The resulting pixel distance is converted into optical distance using the depth sampling calibration for the 1060-nm OCT system and further to the anatomical distance. The segmentation was controlled for manually by an experienced observer. In eyes with nAMD, the segmentation line at the choriocapillaris/retinal pigment epithelium/Bruch's membrane complex sometimes needed manual correction for lesion areas. Therefore, reported variation for automatic segmentation in eyes with pathology is 13%,[30] comparable to values seen by retinal automated segmentation.[31]

Averaging Group Measurement to Obtain Compound Maps

A compound map shows a pixel-wise summary (either by averaging or by using the difference between maps) of the information in each individual thickness map at each location of the map. This image analysis has been described in depth in a previous study.[21] Briefly, to create color-coded compound maps of average thickness, mean and standard deviation of retinal and choroidal thickness was obtained for each group of eyes. The coefficient of variation was used to map contour lines of 45%, 30%, and 15% on the compound map for the variation within each group. Difference maps were generated to investigate the change in thickness by subtracting each group from the other group. A further statistical analysis of the

Investigative Ophthalmology & Visual Science

Investigative Ophthalmology & Visual Science

TABLE. Thickness Measurements for the Retina, Choroid, and Sattler's and Haller's Layer; Age; and Axial Eye Length (AL) Distribution for Different AMD Severities, Mean ± SD (Range)

	Healthy Eyes, $n = 24$	Intermediate AMD Bilateral, $n = 21$	Intermediate AMD of nAMD Fellow Eyes, $n = 22$	nAMD Fellow Eyes, $n = 22$
Foveal thickness, μm	215 ± 18 (173–240)	227 ± 44 (135–336)	233 ± 32 (185–331)	372 ± 179* (201–910)
Subfoveal ChT, μm	259 ± 95 (53–427)	222 ± 98 (81–478)	149 ± 60† (77–313)	171 ± 78‡ (72–346)
Sattler's layer central submacular field	43 ± 36 (1–118)	38 ± 50 (3–189)	18 ± 25§ (0–95)	24 ± 35‖ (0–161)
Sattler's layer total ETDRS field	35 ± 29 (2–95)	31 ± 36 (1–130)	15 ± 20§ (1–77)	18 ± 25‖ (2–118)
Haller's layer central submacular field	123 ± 53 (48–227)	110 ± 60 (54–271)	77 ± 27§ (44–153)	81 ± 28‖ (44–151)
Haller's layer total ETDRS field	110 ± 41 (52–196)	102 ± 49 (55–224)	74 ± 23§ (52–141)	80 ± 26‖ (52–167)
Age, y	75 ± 5 (66–85)	75 ± 4 (67–82)	78 ± 6 (64–89)	-
AL, mm	22.96 ± 0.89 (21.33–25.25)	23.33 ± 0.94 (21.6–24.97)	23.36 ± 0.72 (21.57–24.95)	23.33 ± 0.78 (21.48–24.97)
Visual acuity in logMAR (mean at 20 ft) (range)	0.1 (20/25) (−0.2 to 0.5)	0.1 (20/25) (−0.22 to 0.48)	0.04 (20/21) (−0.16 to 0.48)	0.2 (20/32) (−0.1 to 0.7)

* $P < 0.001$, Wilcoxon signed-rank test between intermediate and the nAMD fellow eyes and Kruskal-Wallis test and post hoc for the difference from intermediate AMD and healthy eyes.
† $P < 0.001$ (one-way ANOVA, post hoc $P < 0.001$ for the difference from healthy eyes and $P < 0.05$ for the difference from intermediate AMD).
‡ $P < 0.001$ (one-way ANOVA, post hoc $P < 0.001$ for the difference from healthy eyes).
§ These sublayers are significantly thinner than healthy and bilateral intermediate AMD sublayers (Kruskal-Wallis test $P < 0.01$).
‖ These sublayers are significantly thinner than healthy ($P < 0.05$, Kruskal-Wallis test and post hoc).

difference between each group was generated by conducting *t*-tests over the field of view. To show areas of statistically significant difference between the compound maps, contour lines for *P* values smaller than 0.05 and 0.001 were drawn on the difference maps. Compound maps for the thickness difference shown in this paper are only the maps with areas of significant statistical difference. For statistical analysis, subfoveal ChT measurement was located beneath the foveola and measured after automatic segmentation and smoothing for compound maps. The statistics software IBM SPSS Statistics for Windows, version 20.0 (IBM Corp., Armonk, NY, USA), was used for conducting ANOVA testing and multiregression analysis of the contribution of groups and their characterizing factors to ChT, Sattler's, and Haller's layers.

Sattler's and Haller's Layer Segmentation

With a novel blood vessel segmentation algorithm, Sattler's and Haller's layer thicknesses were automatically determined.[28,32] The algorithm identifies the voxels that belong to vessels and plots them by the ratio of inner and outer vessels. Outer voxels are neighbored nonvessel voxels. This ratio determines vessel size, and large vessels (large ratio between inner and outer voxels) located closer to the sclera are assigned to Haller's layer while vessels that are located above them and are smaller belong to Sattler's layer. Vessel voxels equal to or below resolution were interpreted as noise. Local variation made measurement analysis of small areas unfeasible, and therefore the sublayer thickness was averaged based on the ETDRS grid that divides the macula into nine subfields. Measurements in AMD eyes have a repeatability variation of 31% in the Haller's layer, which is comparable to those with automatic segmentation in healthy eyes[32] and published manual segmentation methods.[33] When Sattler's layer becomes indistinct in eyes with AMD, the repeatability of the automatic segmentation is decreased.[32] However, clinically, the actual thickness numbers are still within a very small range (e.g., the difference between 4 and 7 μm is 44%, but the absolute values are within a small range). Sattler's and Haller's layer thickness was mapped, and thickness distributions were compared between groups and with fluorescence angiography images of nAMD eyes displaying the CNV location.

RESULTS

All intermediate AMD eyes that were classified as study eyes had multiple drusen within two disc diameters of the fovea. Four of the eyes with intermediate AMD had fellow eyes with only medium-sized drusen (between 63 and 125 μm) within their macular center. Age-related macular degeneration eyes were grouped into intermediate AMD study eyes and non-neovascular fellow eyes ($n = 21$) and intermediate AMD with nAMD fellow eyes ($n = 22$). Control eyes ($n = 24$) were age- and axial eye length–matched healthy eyes (Table). Multiregression analysis showed a significant inverse relationship between age and ChT and between AMD severity and ChT ($R^2 = 0.37$; $P < 0.001$; age: $P < 0.001$, $\beta = -0.43$; axial length: $P > 0.05$; AMD severity: $\beta = -0.31$, $P < 0.01$).

Out of 22 nAMD eyes, 21 displayed reduced Sattler's layer thickness below the CNV location that was identified by fluorescein angiography (Fig. 1). Below the CNV, Haller's layer and choroidal thickness were reduced in relation to the surrounding tissue. Fellow nonneovascular eyes displayed a similar thickness distribution of the choroid, Sattler's, and Haller's layers. Statistical comparison demonstrated that there was no difference between the intermediate AMD and fellow nAMD eyes for the comparison of ChT, Sattler's, and Haller's

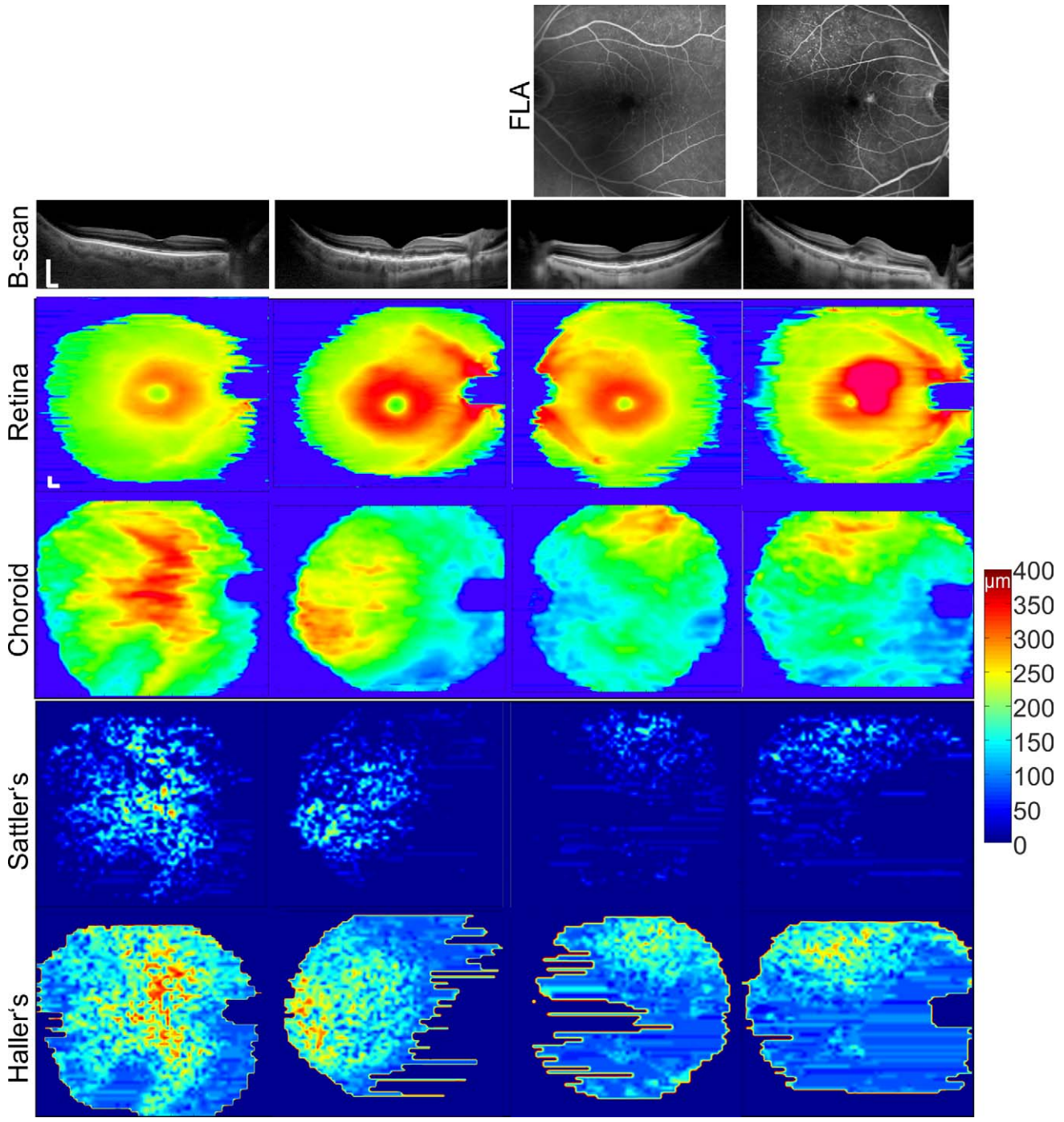

Figure 1. Thickness maps for the retina, choroid, and Sattler's and Haller's layers for representative eyes in each group. Columns from the *left* are a healthy eye and the disease severities: intermediate AMD, intermediate AMD with its nAMD fellow eye. In the healthy eye the choroid and its sublayers are thickest below the macula. *Bar* represents 0.5 mm.

layer thickness ($P > 0.05$, paired *t*-test for ChT and the Wilcoxon signed-rank test for Sattler's and Haller's layers). Choroidal thickness maps from intermediate AMD eyes with nAMD fellow eyes (Fig. 2) displayed a large thinning area throughout the imaged field of view when compared to healthy eyes and significant central, superior, and temporal thinning when compared to intermediate AMD eyes with no nAMD fellow eyes. Measurement of Sattler's and Haller's layer thickness for the central subfield and total ETDRS subfields (Table) exhibited thinner sublayers in intermediate AMD eyes with fellow nAMD eyes when compared to healthy eyes; while in eyes with intermediate AMD with no nAMD fellow eyes, thinning was statistically not significant at any location. Statistical analysis for fellow nAMD eyes revealed significantly thinner subfoveal choroid, Sattler's, and Haller's layer than in healthy eyes (Table).

Discussion

Choroidal vasculature has a distinct segmental nature,[34] and enlarged choroidal watershed zones representing choroidal

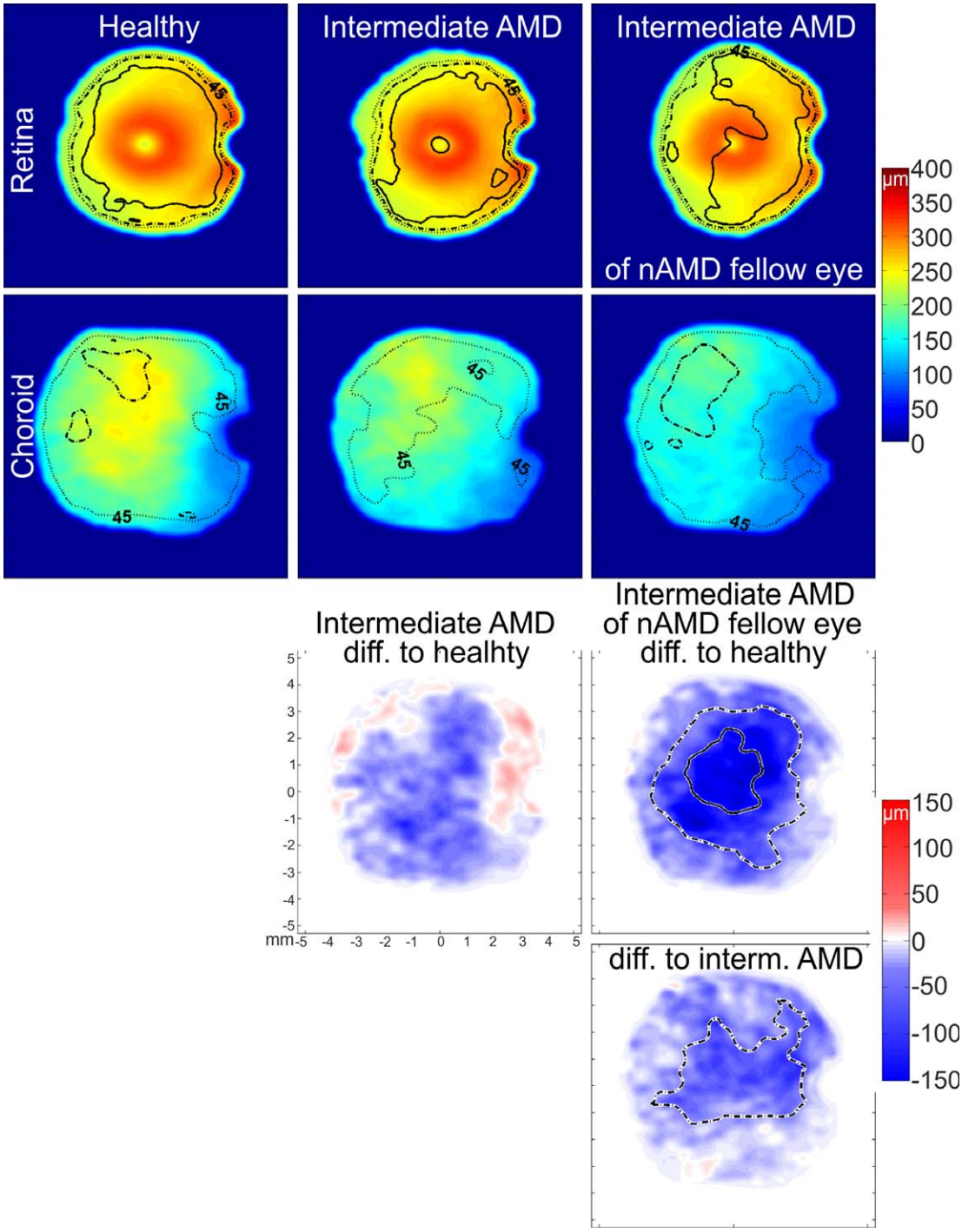

Figure 2. Compound thickness maps for the retina and the choroid and their respective difference maps for the three disease groups. Numbers of averaged eyes are given in the Table. Thickness maps display *contour lines* for 45% (*dotted*), 30% (*broken*), and 15% (*solid*) coefficient of variation. Difference maps for the choroidal thickness of each disease group and the healthy eyes and for choroidal thickness between both intermediate AMD groups demonstrate the location of significant difference between groups found by post hoc testing. *Broken* and *solid contour lines* represent significant differences of $P < 0.05$ and $P < 0.001$, respectively.

topographical changes are a possible determinant of the neovascularization location.[35] This study found, by using choroidal, Sattler's, and Haller's layer thickness maps, an altered thickness distribution across the group of intermediate AMD with nAMD fellow eyes and the nAMD eyes. In the intermediate AMD group and their fellow nAMD eyes, Sattler's layer thickness was markedly reduced when compared to normal. There was reduced thickness below the neovascularization in the nAMD eyes.

A limitation of this study was the large variation inherent to vessel morphology and its automatic segmentation. There are no clear boundaries between the choriocapillaris, Sattler's layer, and Haller's layer. To overcome this morphologic challenge, the automated segmentation used a relative vessel

Investigative Ophthalmology & Visual Science

size threshold and assigned the largest vessel within a $1^\circ \times 1^\circ$ volume to Haller's and any vessels above it to Sattler's layer.[28,32] Gaps between vessels can be interpolated by manual segmentation; but automated segmentation measures no thickness between vessels, so that a large variation is present within individual maps. Instead of using local measurements that are subject to variation, averaging measurements across subfields of the ETDRS grid is recommended.[32] To the best of our knowledge, this is the first study to attribute choroidal thinning in AMD to Sattler's and Haller's layer and to find the strongest association between neovascularization and Sattler's layer. The reduced sublayer thickness may be due to decreased vessel density and/or to tissue shrinkage. Many histologic studies that have investigated the choroid and its vasculature have mainly demonstrated choriocapillaris dropout.[14–16] It has been indicated that larger choroidal vessel density may also be reduced.[36] Despite the large variation in the results of this study, Sattler's layer relative thinning is more apparent than Haller's layer thinning. This may reflect the same process that is affecting the neighboring choriocapillaris.

Age-related macular degeneration presents with disease alterations of the retinal photoreceptors, retinal pigment epithelium, Bruch's membrane, and the choroid in its different phenotypes. Recent research is focusing on the differentiation of possible phenotypes to understand the disease pathways. Further, a complete understanding of AMD types and changes with each stage may help to support genotype-based analysis and the development of individual phenotype-directed treatments. Choroidal thickness measurement has been important to assist differentiation of retinal diseases such as the diagnosis of acquired vitelliform lesions that may present with a thickened choroid in contrast to late AMD that decreases ChT.[12] Geographic atrophy is closely related to choroidal thickness alteration.[37] Subretinal drusenoid deposits are related to a thickened choroid underneath them,[38,39] but their presence may lead to a more severe subfoveal choroidal thinning.[40,41] Not differentiating AMD stages and not excluding AMD phenotypes that increase choroidal thickness may cause noise in choroidal thickness measurement and erroneously result in no choroidal thickness change in AMD eyes.[42] To ensure homogeneity of the groups, this study excluded phenotypes with known changes to the choroid such as subretinal deposits and polypoidal lesions. Subretinal deposits have been found to affect the outer retina,[43] increase choroidal and Sattler's layer thickness located underneath them, and reduce subfoveal choroidal thickness in comparison to eyes with no subretinal deposits.[38,39] Subretinal deposits sometimes have a subtle appearance and may be overlooked by one examination alone.[44] Optical coherence tomography imaging for clarification of retinal changes has been recommended by other investigators[44,45]; and in this study, seven initially included subjects had to be excluded from the analysis after OCT images were examined over a large field of view. However, subretinal deposits and acquired vitelliform lesions can disappear with time,[43,45] and there is a possibility that study eyes of each group had them prior to inclusion in this study.

In conclusion, this study investigated the difference in choroidal thickness and vascular sublayers between healthy subjects and groups of patient eyes that had bilateral intermediate AMD or a fellow eye with nAMD. Therefore the groups of patient eyes with intermediate AMD possessed major risk factors for developing late AMD such as advanced age, large drusen, and pigmentary changes. Their only difference was the AMD stage in the fellow eye, which is another major risk factor for developing AMD.[20] Choroidal, Sattler's, and Haller's layer thickness decrease correlated between intermediate AMD eyes consisting of large drusen and pigmentation change and the nAMD eyes of the same patients. Choroidal and choroidal sublayer thicknesses of these eyes differed significantly from values in healthy eyes while thicknesses of bilateral intermediate AMD eyes were not different from those in healthy eyes. This choroidopathy may reflect a part of the pathophysiology of the late AMD form.

Acknowledgments

The authors thank Boris Hermann, PhD, Behrooz Zabihian, MSc, and the staff of the Medical Retina Unit at the Rudolf Foundation Clinic for their valuable support throughout the study.

Supported in part by Medical University Vienna; Oesterreichische Nationalbank (Jubilaeumsfond, Project 14294); Macular Vision Research Foundation, United States; FAMOS (FP7 ICT 317744); FWF-NFN (Photoacoustic Imaging in Biology and Medicine); National Institutes of Health Grant R01-EY011289-27; Carl Zeiss Meditec, Inc.; Femtolasers GmbH; the Christian Doppler Society (Christian Doppler Laboratory [Laser Development and Their Application in Medicine]); German Research Foundation DFG-HO-1791/11-1, DFG Training Group 1773 (Heterogeneous Image Systems); and Erlangen Graduate School of Advanced Optical Technologies.

Disclosure: **M. Esmaeelpour**, None; **S. Ansari-Shahrezaei**, None; **C. Glittenberg**, Carl Zeiss Meditec (C); **S. Nemetz**, None; **M.F. Kraus**, Optovue (I), P; **J. Hornegger**, Optovue (I), P; **J.G. Fujimoto**, Optovue (I), P; **W. Drexler**, Carl Zeiss Meditec (C); **S. Binder**, None

References

1. Friedman DS, O'Colmain BJ, Muñoz B, et al. Prevalence of age-related macular degeneration in the United States. *Arch Ophthalmol*. 2004;122:564–572.
2. Klein R, Klein BEK, Knudtson MD, Meuer SM, Swift M, Gangnon RE. Fifteen-year cumulative incidence of age-related macular degeneration: the Beaver Dam Eye Study. *Ophthalmology*. 2007;114:253–262.
3. Korb CA, Kottler UB, Wolfram C, et al. Prevalence of age-related macular degeneration in a large European cohort: results from the population-based Gutenberg Health Study. *Graefes Arch Clin Exp Ophthalmol*. 2014. doi:10.1007/s00417-014-2591-9.
4. Jia Y, Bailey ST, Wilson DJ, et al. Quantitative optical coherence tomography angiography of choroidal neovascularization in age-related macular degeneration. *Ophthalmology*. 2014;121:1435–1444.
5. Hayreh SS. Submacular choroidal vascular pattern. Experimental fluorescein fundus angiographic studies. *Albrecht Von Graefes Arch Klin Exp Ophthalmol*. 1974;192:181–196.
6. Mokwa NF, Ristau T, Keane PA, Kirchhof B, Sadda SR, Liakopoulos S. Grading of age-related macular degeneration: comparison between color fundus photography, fluorescein angiography, and spectral domain optical coherence tomography. *J Ophthalmol*. 2013;2013:385915.
7. Regatieri CV, Branchini L, Duker JS. The role of spectral-domain OCT in the diagnosis and management of neovascular age-related macular degeneration. *Ophthalmic Surg Lasers Imaging*. 2011;42(suppl):S56–S66.
8. Krebs I, Glittenberg C, Hagen S, Haas P, Binder S. Retinal angiomatous proliferation: morphological changes assessed by Stratus and Cirrus OCT. *Ophthalmic Surg Lasers Imaging*. 2009;40:285–289.
9. Wood A, Binns A, Margrain T, et al. Retinal and choroidal thickness in early age-related macular degeneration. *Am J Ophthalmol*. 2011;152:1030–1038.
10. Margolis R, Spaide RF. A pilot study of enhanced depth imaging optical coherence tomography of the choroid in normal eyes. *Am J Ophthalmol*. 2009;147:811–815.

11. Ikuno Y, Kawaguchi K, Nouchi T, Yasuno Y. Choroidal thickness in healthy Japanese subjects. *Invest Ophthalmol Vis Sci*. 2010;51:2173–2176.
12. Coscas F, Puche N, Coscas G, et al. Comparison of macular choroidal thickness in adult onset foveomacular vitelliform dystrophy and age-related macular degeneration. *Invest Ophthalmol Vis Sci*. 2014;55:64–69.
13. Sohn EH, Khanna A, Tucker BA, Abràmoff MD, Stone EM, Mullins RF. Structural and biochemical analyses of choroidal thickness in human donor eyes. *Invest Ophthalmol Vis Sci*. 2014;55:1352–1360.
14. Ramrattan RS, van der Schaft TL, Mooy CM, de Bruijn WC, Mulder PG, de Jong PT. Morphometric analysis of Bruch's membrane, the choriocapillaris, and the choroid in aging. *Invest Ophthalmol Vis Sci*. 1994;35:2857–2864.
15. Bhutto I, Lutty G. Understanding age-related macular degeneration (AMD): relationships between the photoreceptor/retinal pigment epithelium/Bruch's membrane/choriocapillaris complex. *Mol Aspects Med*. 2012;33:295–317.
16. Bird AC, Phillips RL, Hageman GS. Geographic atrophy: a histopathological assessment. *JAMA Ophthalmol*. 2014;132:338–345.
17. Mullins RF, Johnson MN, Faidley EA, Skeie JM, Huang J. Choriocapillaris vascular dropout related to density of drusen in human eyes with early age-related macular degeneration. *Invest Ophthalmol Vis Sci*. 2011;52:1606–1612.
18. Buch H, Nielsen NV, Vinding T, Jensen GB, Prause JU, la Cour M. 14-year incidence, progression, and visual morbidity of age-related maculopathy: the Copenhagen City Eye Study. *Ophthalmology*. 2005;112:787–798.
19. Wang JJ, Rochtchina E, Lee AJ, et al. Ten-year incidence and progression of age-related maculopathy: the Blue Mountains Eye Study. *Ophthalmology*. 2007;114:92–98.
20. Chew EY, Clemons TE, Agrón E, et al. Ten-year follow-up of age-related macular degeneration in the age-related eye disease study: AREDS report no. 36. *JAMA Ophthalmol*. 2014;132:272–277.
21. Esmaeelpour M, Povazay B, Hermann B, et al. Three-dimensional 1060-nm OCT: choroidal thickness maps in normal subjects and improved posterior segment visualization in cataract patients. *Invest Ophthalmol Vis Sci*. 2010;51:5260–5266.
22. Unterhuber A, Považay B, Hermann B, Sattmann H, Chavez-Pirson A, Drexler W. In vivo retinal optical coherence tomography at 1040 nm-enhanced penetration into the choroid. *Opt Express*. 2005;13:3252–3258.
23. Ferris FL III, Wilkinson CP, Bird A, et al. Clinical classification of age-related macular degeneration. *Ophthalmology*. 2013;120:844–851.
24. Age-Related Eye Disease Research Study Group. The Age-Related Eye Disease Study system for classifying age-related macular degeneration from stereoscopic color fundus photographs: the Age-Related Eye Disease Study Report Number 6. *Am J Ophthalmol*. 2001;132:668–681.
25. ANSI. *Safe Use of Lasers & Safe Use of Optical Fiber Communications*. American National Standard Institute - Z136 Committee; 2000:168.
26. ICNIRP. *Revision of the Guidelines on Limits of Exposure to Laser radiation of wavelengths between 400nm and 1.4μm*. International Commission on Non-Ionizing Radiation Protection; 2000:431–440.
27. Povazay B, Hermann B, Hofer B, et al. Wide-field optical coherence tomography of the choroid in vivo. *Invest Ophthalmol Vis Sci*. 2009;50:1856–1863.
28. Kajić V, Esmaeelpour M, Glittenberg C, et al. Automated three-dimensional choroidal vessel segmentation of 3D 1060 nm OCT retinal data. *Biomed Opt Express*. 2012;4:134–150.
29. Kraus MF, Potsaid B, Mayer MA, et al. Motion correction in optical coherence tomography volumes on a per A-scan basis using orthogonal scan patterns. *Biomed Opt Express*. 2012;3:1182–1199.
30. Kajić V, Esmaeelpour M, Považay B, Marshall D, Rosin PL, Drexler W. Automated choroidal segmentation of 1060 nm OCT in healthy and pathologic eyes using a statistical model. *Biomed Opt Express*. 2011;3:86–103.
31. Kajić V, Povazay B, Hermann B, et al. Robust segmentation of intraretinal layers in the normal human fovea using a novel statistical model based on texture and shape analysis. *Opt Express*. 2010;18:14730–14744.
32. Esmaeelpour M, Kajic V, Zabihian B, et al. Choroidal Haller's and Sattler's layer thickness measurement using 3-dimensional 1060-nm optical coherence tomography. *PLoS One*. 2014. doi: 10.1371/journal.pone.0099690.
33. Sim DA, Keane PA, Mehta H, et al. Repeatability and reproducibility of choroidal vessel layer measurements in diabetic retinopathy using enhanced depth optical coherence tomography. *Invest Ophthalmol Vis Sci*. 2013;54:2893–2901.
34. Hayreh SS. In vivo choroidal circulation and its watershed zones. *Eye*. 1990;4(pt 2):273–289.
35. Mendrinos E, Pournaras CJ. Topographic variation of the choroidal watershed zone and its relationship to neovascularization in patients with age-related macular degeneration. *Acta Ophthalmol*. 2009;87:290–296.
36. Spraul CW, Lang GE, Grossniklaus HE, Lang GK. Histologic and morphometric analysis of the choroid, Bruch's membrane, and retinal pigment epithelium in postmortem eyes with age-related macular degeneration and histologic examination of surgically excised choroidal neovascular membranes. *Surv Ophthalmol*. 1999;44(suppl 1):S10–S32.
37. Lee JY, Lee DH, Lee JY, Yoon YH. Correlation between subfoveal choroidal thickness and the severity or progression of nonexudative age-related macular degeneration. *Invest Ophthalmol Vis Sci*. 2013;54:7812–7818.
38. Querques G, Querques L, Forte R, Massamba N, Coscas F, Souied EH. Choroidal changes associated with reticular pseudodrusen. *Invest Ophthalmol Vis Sci*. 2012;53:1258–1263.
39. Haas P, Esmaeelpour M, Ansari-Shahrezaei S, Drexler W, Binder S. Choroidal thickness in patients with reticular pseudodrusen using 3D 1060-nm OCT maps. *Invest Ophthalmol Vis Sci*. 2014;55:2674–2681.
40. Switzer DW Jr, Mendonça LS, Saito M, Zweifel SA, Spaide RF. Segregation of ophthalmoscopic characteristics according to choroidal thickness in patients with early age-related macular degeneration. *Retina*. 2012;32:1265–1271.
41. Sigler EJ, Randolph JC. Comparison of macular choroidal thickness among patients older than age 65 with early atrophic age-related macular degeneration and normals. *Invest Ophthalmol Vis Sci*. 2013;54:6307–6313.
42. Jonas JB, Forster TM, Steinmetz P, Schlichtenbrede FC, Harder BC. Choroidal thickness in age-related macular degeneration. *Retina*. 2014;34:1149–1155.
43. Spaide RF. Outer retinal atrophy after regression of subretinal drusenoid deposits as a newly recognized form of late age-related macular degeneration. *Retina*. 2013;33:1800–1808.
44. Ueda-Arakawa N, Ooto S, Tsujikawa A, Yamashiro K, Oishi A, Yoshimura N. Sensitivity and specificity of detecting reticular pseudodrusen in multimodal imaging in Japanese patients. *Retina*. 2013;33:490–497.
45. Freund KB, Laud K, Lima LH, Spaide RF, Zweifel S, Yannuzzi LA. Acquired vitelliform lesions: correlation of clinical findings and multiple imaging analyses. *Retina*. 2011;31:13–25.

Investigative Ophthalmology & Visual Science